

# Electron Emission Effects in Bounded and Dusty Plasma

Igor D. Kaganovich for PPPL group:

Y. Raitses, A. Khrabrov, D. Sydorenko, P. Dourbal, A. Merzhevsky, + many students and visitors

*Princeton Plasma Physics Laboratory*

*Princeton, NJ 08543*



# Outline

---

- **Motivation and applications**
- **Effects of emission on sheath**
- **Emission from complex surfaces**
- **Effect of clean vs “dirty” surface on secondary electron emission yield**
- **Two-stream instability in bounded plasmas**

# Outline

---

- **Motivation and applications**
  - Effects of emission on sheath
  - Emission from complex surfaces
    - Effect of clean vs “dirty” surface on SEY
    - Two-stream instability in bounded plasmas

**Any plasma with electron temperatures above 20 eV for dielectric walls, and above 50-100 eV for metal walls is subject to strong secondary electron emission (SEE) effects:**

---

**Hall thrusters and Helicon thrusters**

**Hollow cathodes for high power microwave electronics**

**Multipactor breakdown and surface discharges**

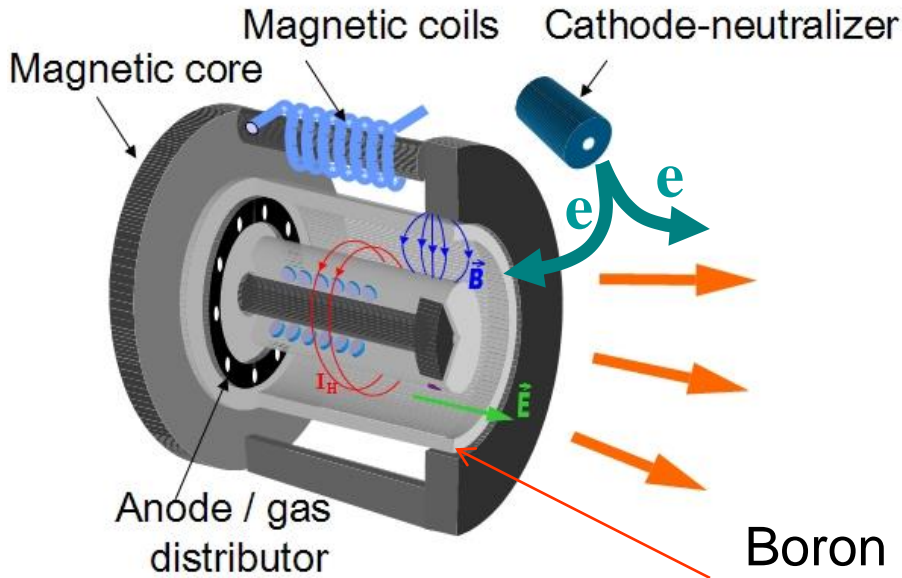
**Space plasmas and dusty plasmas**

**Fusion plasmas**

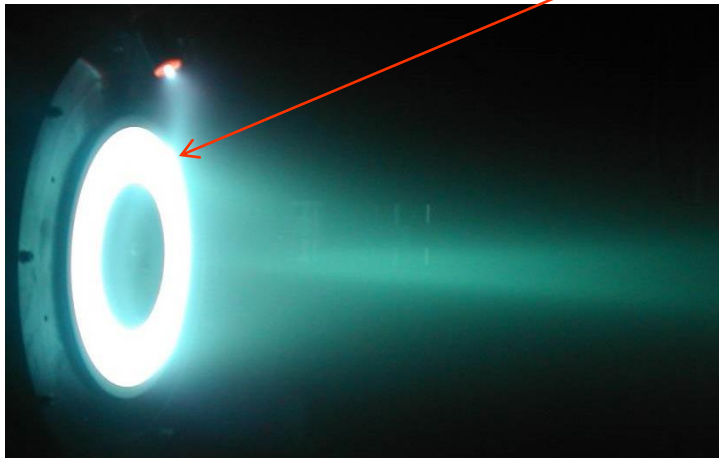
**Plasma processing discharges with RF or DC bias**

- **Strong secondary electron emission from the floating walls can alter plasma-wall interaction and change plasma properties.**
- **Strong SEE can significantly increase electron heat flux from plasma to the wall leading to: 1) wall heating and evaporation and 2) plasma cooling.**

# Hall Thruster (HT) – fuel-efficient plasma propulsion device for space applications



Boron nitride ceramic channel



*Diameter* ~ 1 -100 cm  
*Working gases:* Xe, Kr  
*Pressure* ~  $10^{-4}$  torr  
*Power* ~ 0.1- 50 kW

*Thrust* ~  $10^{-3}$  - 1N  
*Isp* ~ 1000-3000 sec  
*Efficiency* up to 70%

✓ Hall thrusters can produce much higher thrust densities than ion thrusters

**One slide summary of  
AFSOR project on effects of SEE emission**

# Effects of Electron-Induced Secondary Electron Emission (SEE) on Plasma-Wall Interactions

Yevgeny Raitses and Igor Kaganovich

**Status quo:** Plasma with a strong SEE is relevant to plasma thrusters, high power MW devices, etc. Strong SEE can significantly alter plasma-wall interaction affecting thruster performance and lifetime. The observed SEE effects in thrusters requires fully kinetic modeling of plasma-wall interaction.

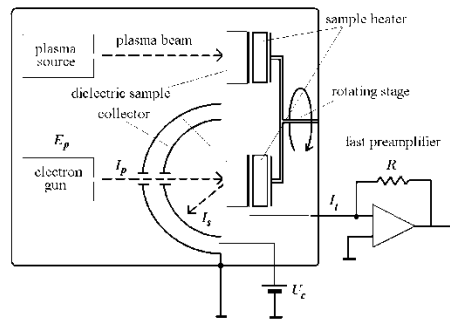
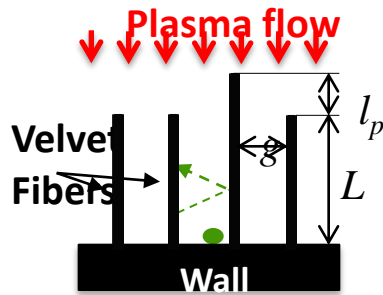
**New insight:** Engineered materials with surface architecture can be used to control and suppress SEE.

**Project goal:** Characterize effects of surface architecture on SEE and plasma-wall interaction

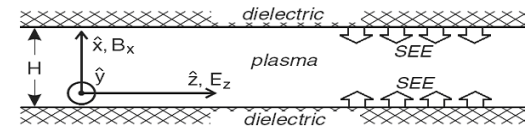
## Main accomplishments

Surface architecture of engineered materials may induce undesired electron field emission

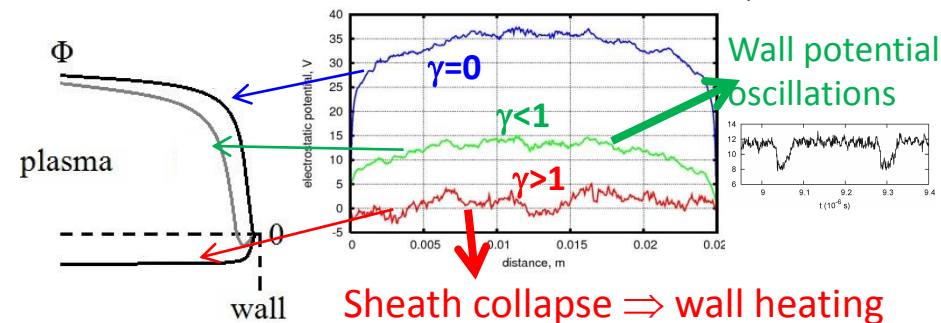
How it works:  $\gamma \approx 0$



Kinetic modeling predict new plasma regimes with strong SEE: unstable sheath, sheath collapse



Three regimes for different effective SEE yield,  $\gamma$



IEPC papers: 131, 132, 175, 176, 239, 307, 313, 320, 360, 390, 400

### Key recent publications

Phys. Rev. Lett. **108**, 235001 and 255001 (2012);  
 Phys. Plasmas **19**, 123513 and 093511 (2012);  
 Phys. Rev. Lett. **111**, 075002 and 115002 (2013).

# **Brief summary of previous results on effects of SEE emission**

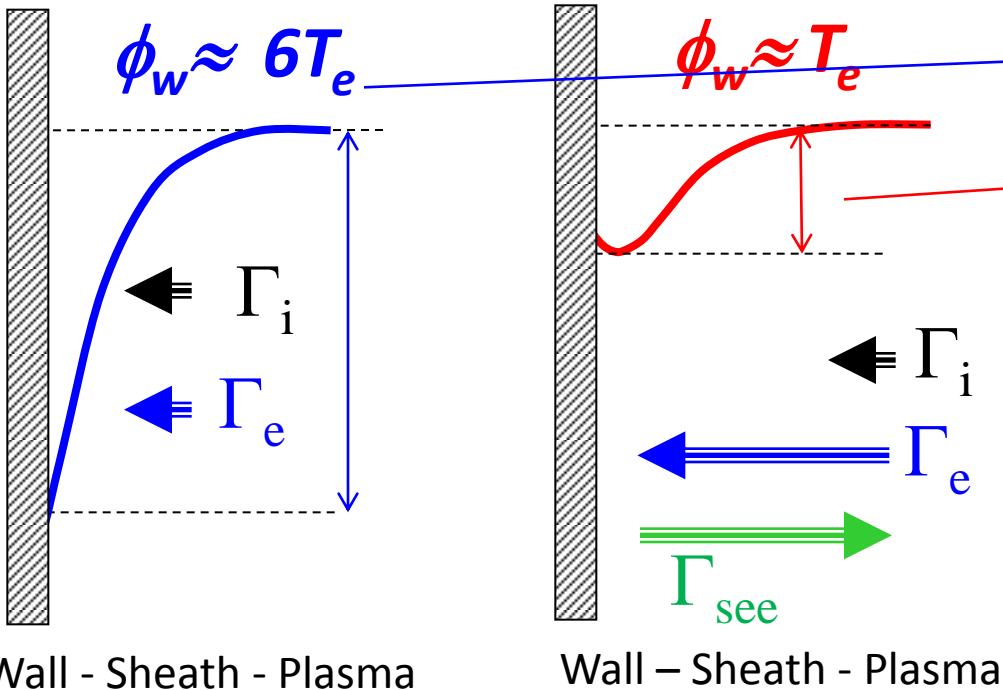
# Outline

---

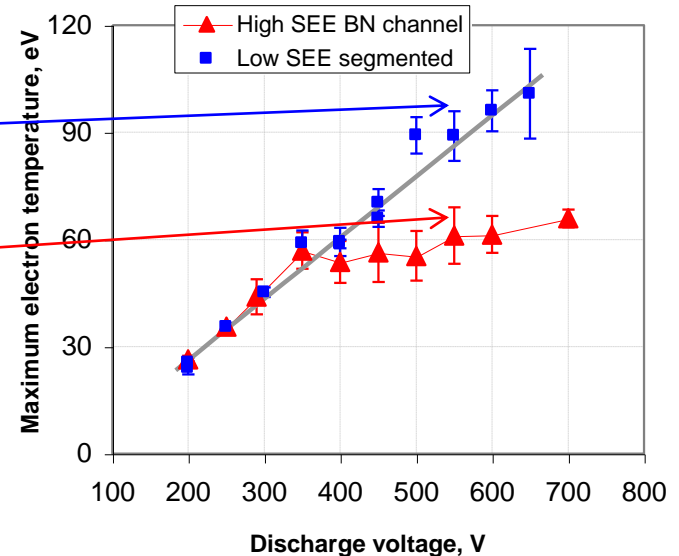
- Motivation and applications
- **Effects of emission on sheath**
- Emission from complex surfaces
- Effect of clean vs “dirty” surface on SEY
- Two-stream instability in bounded plasmas

# Electron emission from the wall can increase the plasma heat flux to the wall many times

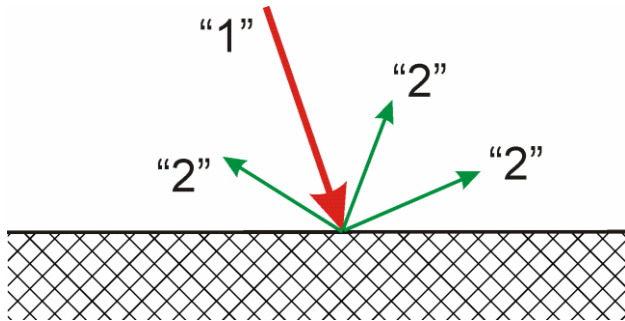
- Without SEE, sheath of space charge near the wall reflects most electrons back to the plasma, thus effectively insulating wall from the plasma (Left Figure)
- SEE reduces the wall potential and allows large electron flux to the wall (Right Figure)



Hall thruster experiments show very different maximum electron temperatures with high and low SEE channel wall materials



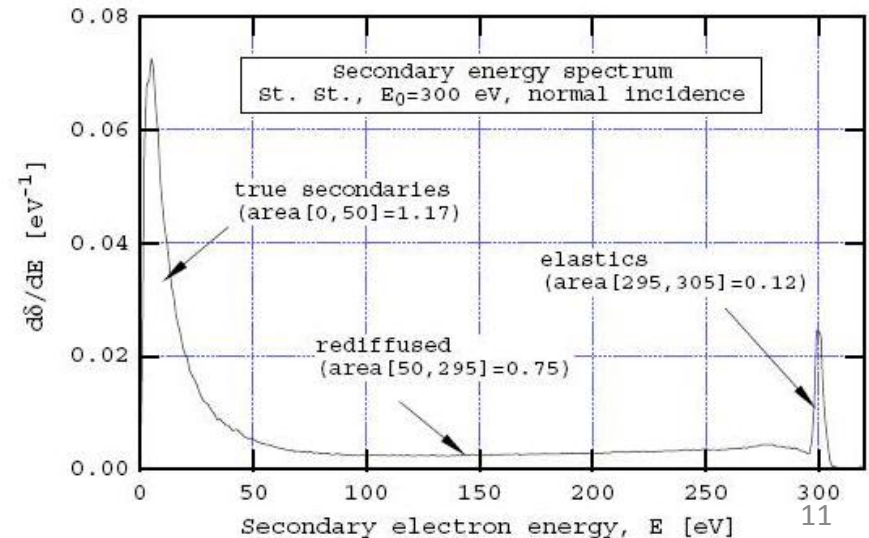
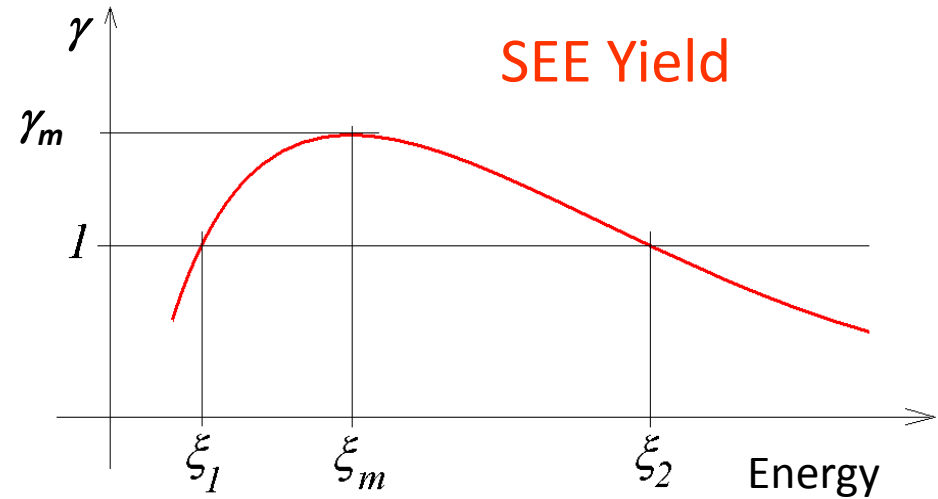
# Electron-induced secondary electron emission (SEE)



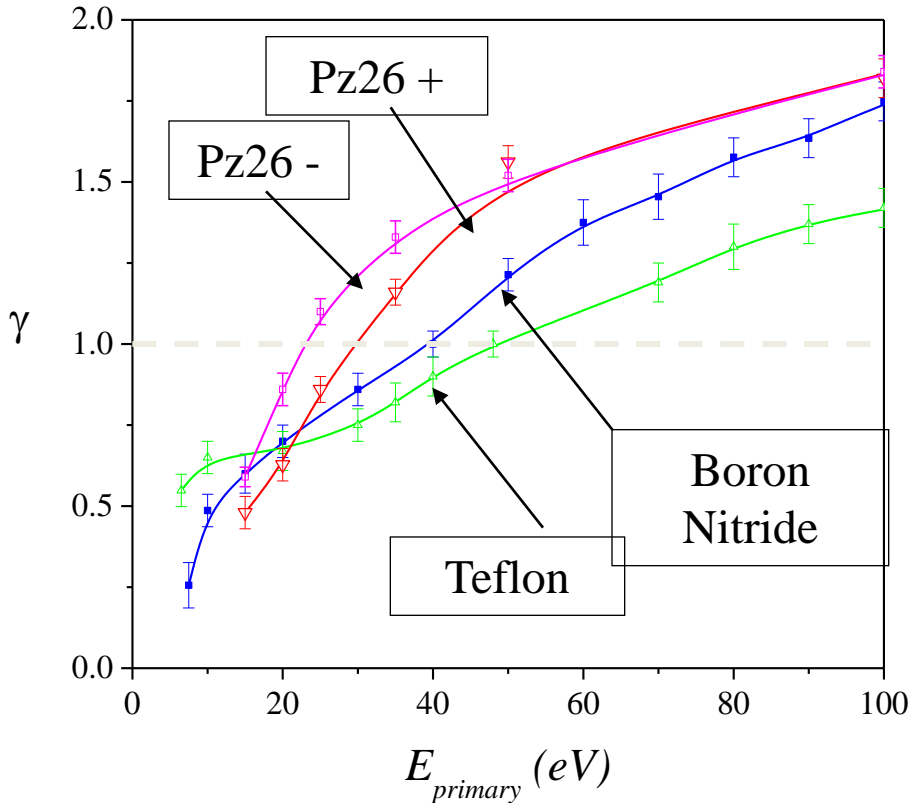
SEE yield  $\gamma = \frac{\text{Secondaries}}{\text{Primaries}}$

$$\gamma = \gamma(E_e)$$

Example of energy spectrum  
(for steel) 



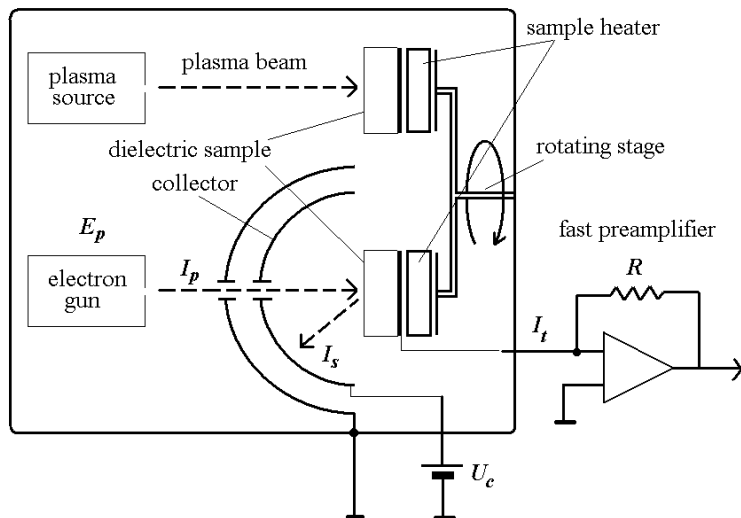
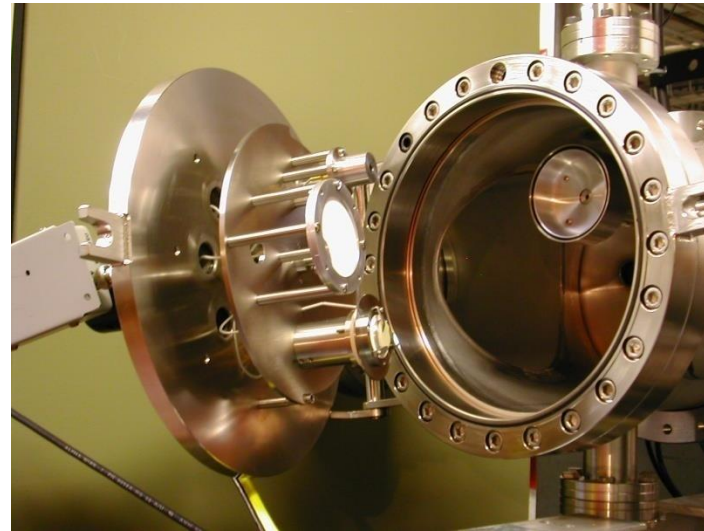
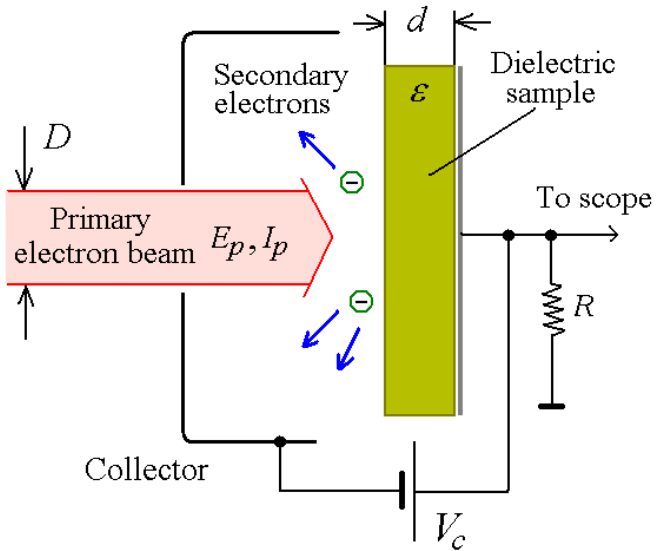
# Secondary electron emission yield from dielectric materials



**Note:**  
for Boron Nitride ceramic, if plasma (primary) electrons have Maxwellian electron energy distribution function (EEDF):

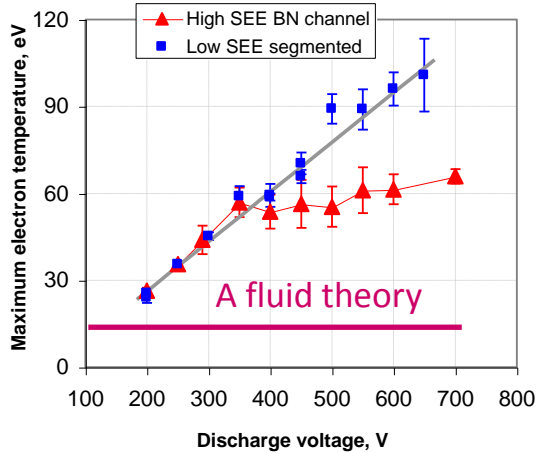
$$\chi(T_e) = 1 \text{ at } T_e = 18.3 \text{ eV}$$

# Upgraded setup for measurements of SEE yield from micro-engineered materials



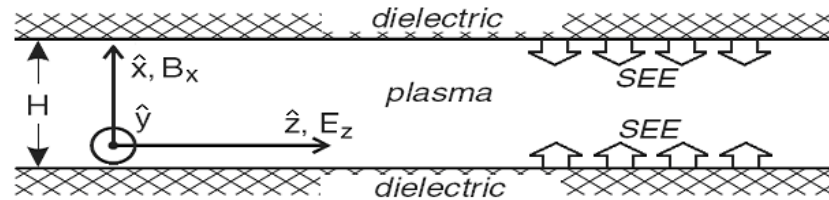
- Cryogenic system to maintain better vacuum ( $<10^{-8}$  torr) during SEE measurements
- Ion source to remove surface charges
- The upgrade allows to minimize, outgassing, surface, contamination, etc.

# For many plasma applications, electron heat flux to the wall needs to be calculated kinetically

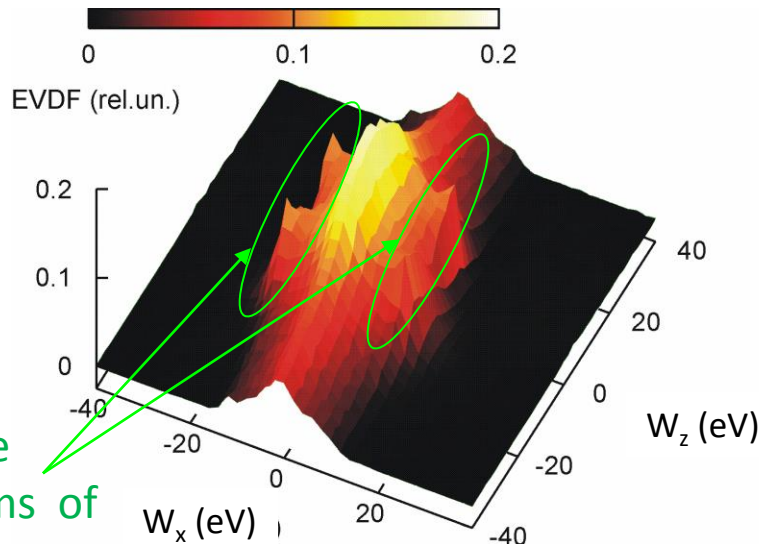


Large quantitative disagreement between experiments and fluid theories for predictions of the electron temperature in Hall thrusters

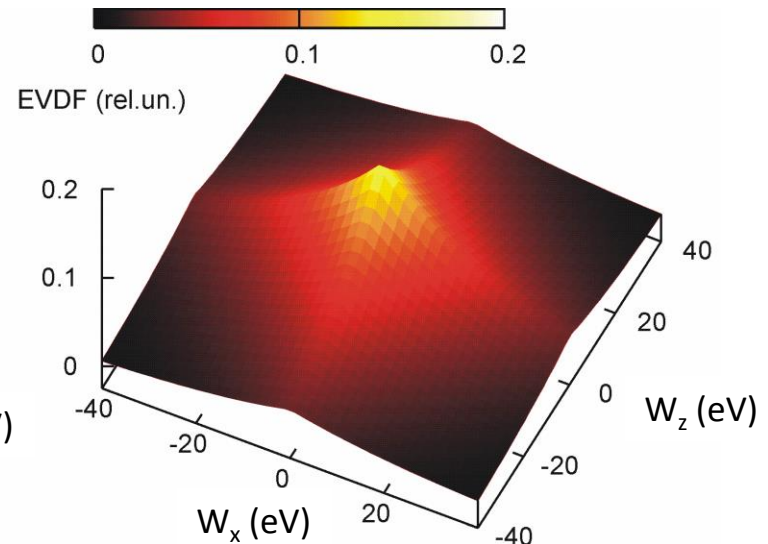
*Y. Raitses et al., Phys. Plasmas 2006*  
*I. Kaganovich et al., Phys. Plasmas 2007*



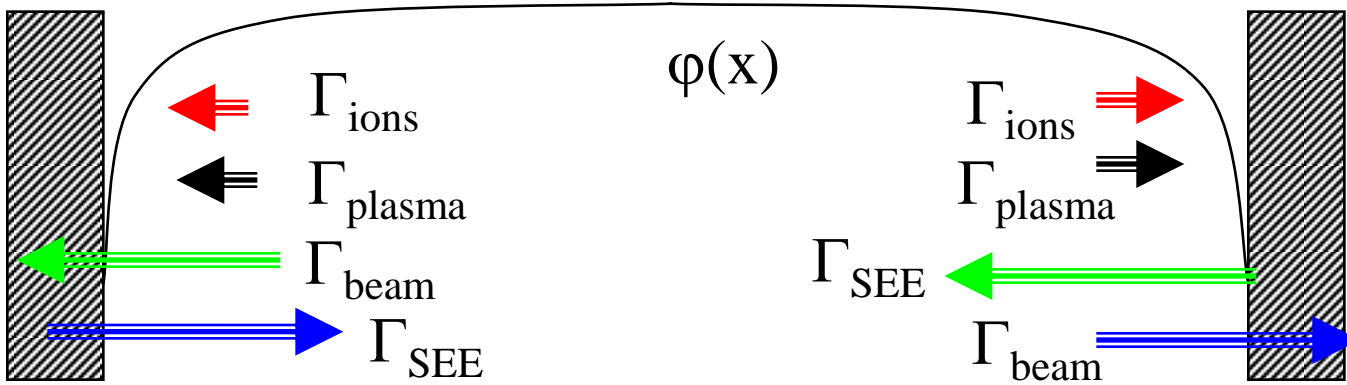
## Hall thruster plasma, 2D-EVDF



## Isotropic Maxwellian plasma, 2D-EVDF



# Electron fluxes have several components, including plasma bulk electrons, and counter-streaming beams of SEE electrons from walls



H. Wang, et al, J. Appl. Phys. D. 47, 2014.

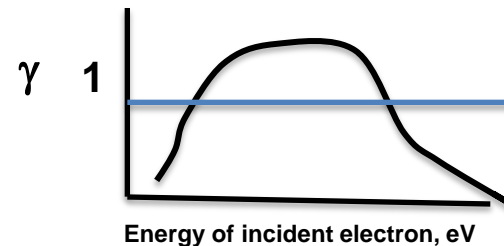
Net secondary electron emission  $\gamma_{net}$  accounts for kinetic effects by separating SEE yield of plasma ( $\gamma_p$ ) and beam electrons ( $\gamma_b$ )

Note:  $\gamma_{net} > 1$  if  $\gamma_b > 1$

Total emission coefficient:

$$\gamma_{net} \approx \frac{\gamma_p}{1 + (\gamma_p - \gamma_b)}$$

SEE Yield as function of incident electron energy

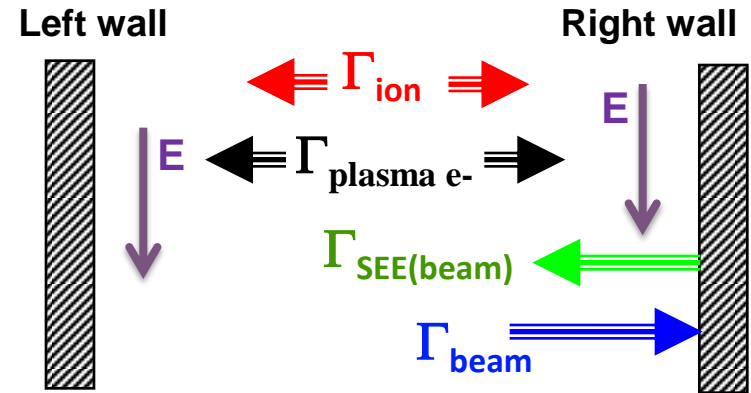
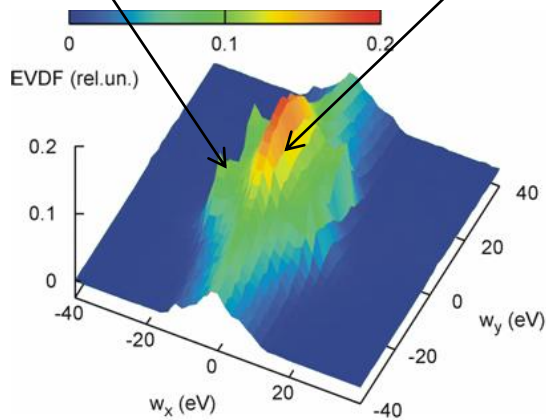


# Particle-in-cell (PIC) simulations of plasma in Hall thrusters

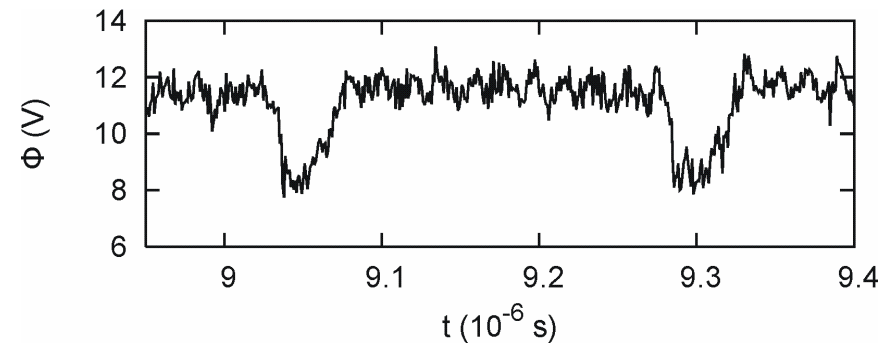
12 cm diameter  
2 kW Hall thruster



Sheath oscillations occur due to coupling of the sheath potential and non-Maxwellian electron energy distribution function with intense electron beams emitted from the walls.



Plasma potential as a function of time

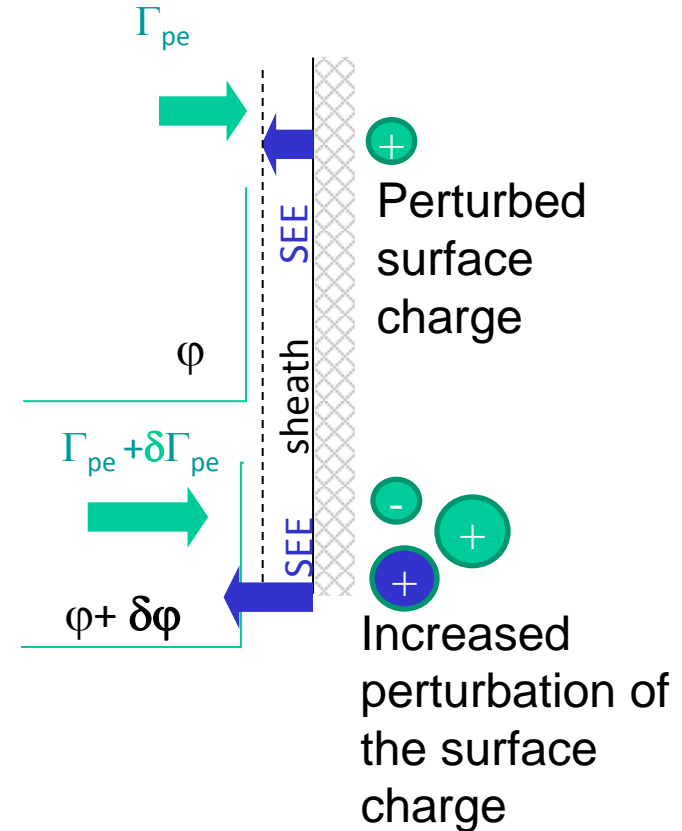


# Criterion for onset of sheath oscillations in the presence of strong SEE

Obtained analytical criterion for sheath instability,  $dJ/d\phi > 0 \Rightarrow \gamma_{w=\phi} > 1$ .

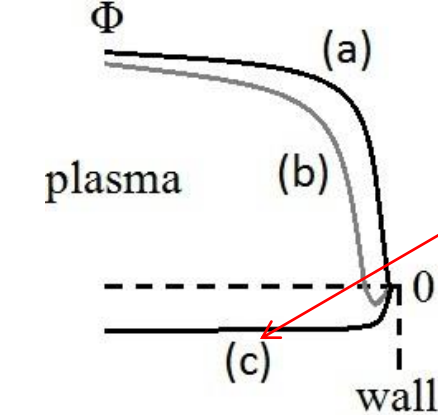
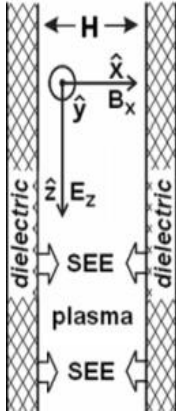
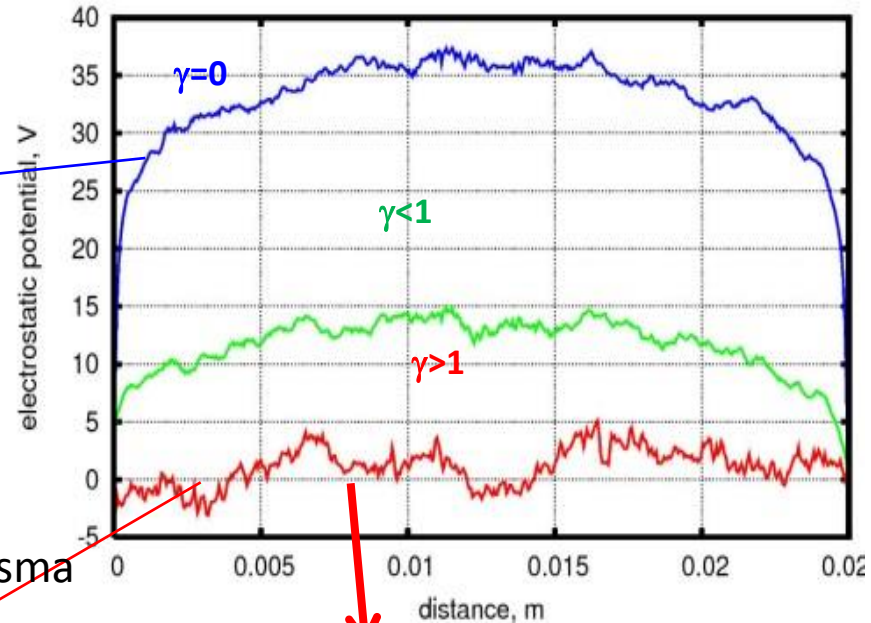
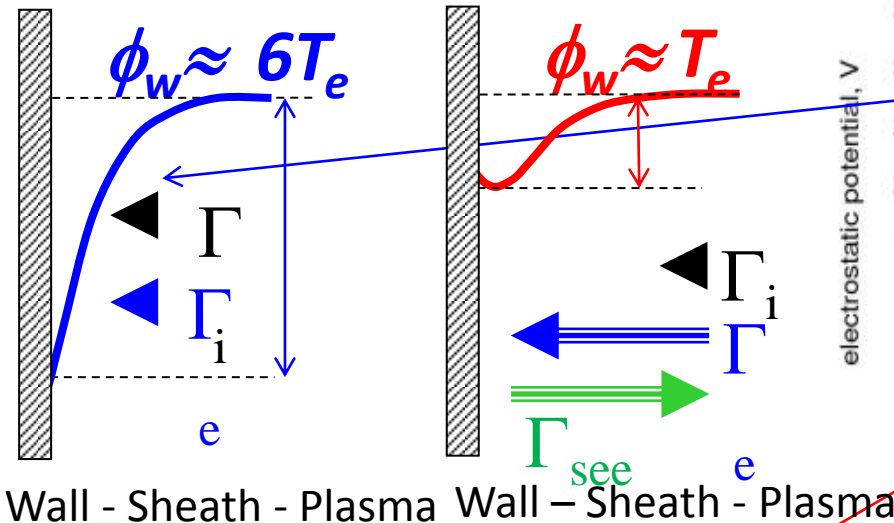
If sheath potential decreases due to positive charge fluctuations on the wall ( $\delta\phi$ ), the incident electron flux increases. If secondary electron emission coefficient of additionally released electrons  $\gamma_{w=\phi} > 1$ , the emitted electron fluxes increases more than incident flux and wall charges more positively instead of restoring to the original wall charge.

## Schematic of instability



# New regimes of plasma-wall interaction with a very strong SEE, $\gamma > 1$

PIC simulations reveal three regimes for different effective SEE yield,  $\gamma$ ;  
 A. Khrabrov  $\sim$ (2010). **Due to nonMaxwellian EEDF, SCL theory does not apply.**



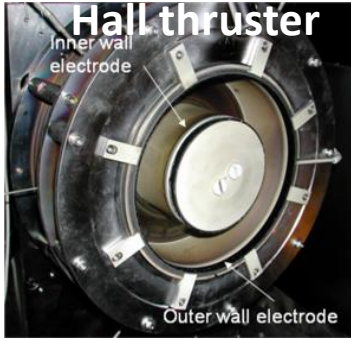
- SEE electrons acquire enough energy from the electric field parallel to the wall causing  $\gamma = 1$
- Sheath collapse leads to extreme wall heating by plasma and plasma losses

# Outline

---

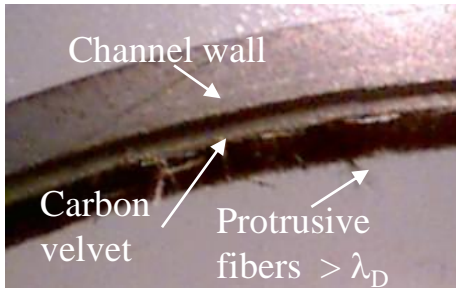
- Motivation and applications
- Effects of emission on sheath
- **Emission from complex surfaces**
  - Effect of clean vs “dirty” surface on SEY
  - Two-stream instability in bounded plasmas

# Plasma properties can be changed by applying engineered materials to the surface

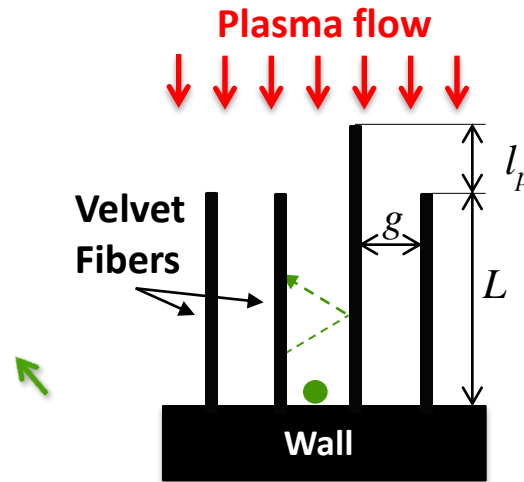


Application of carbon velvet to channel walls improves considerably thruster performance by reducing the electron cross-field current and by increasing nearly twice the maximum electric field in the channel compared with the conventional BN ceramic walls.

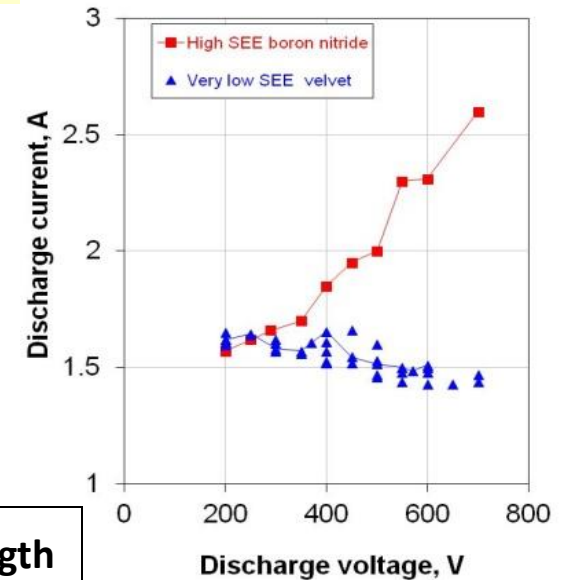
Velvet before plasma



Plasma burned out all protrusive fibers



To avoid field emission  $g, l_p < \text{Debye length}$



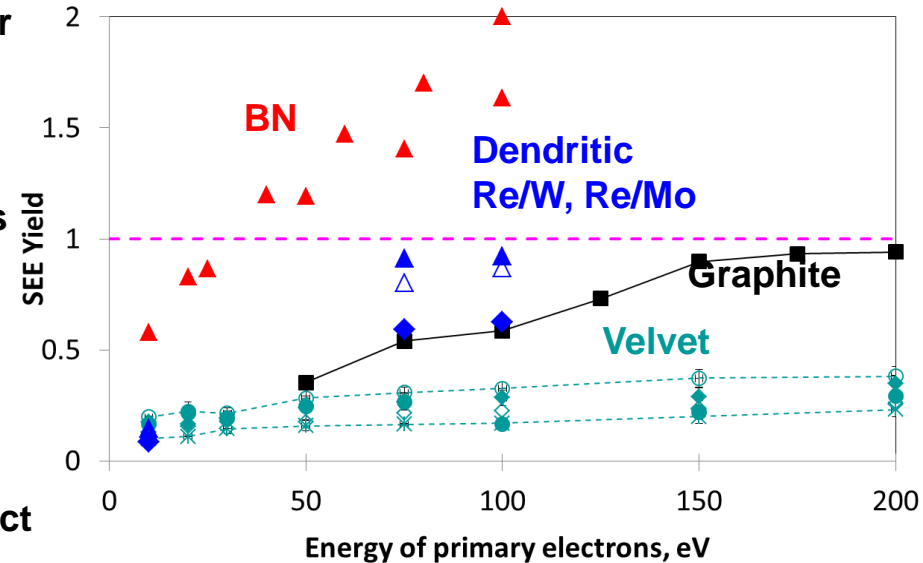
- Velvet suppresses SEE and reduces current at high voltages (good)
  - Sharp tips can enhance field emission leading to arcing (bad)
  - Need to engineer velvet morphology so that inter fiber gaps and protrusions are located well inside the sheath to avoid damage by arcing
- Need to take into account spatial and temporal variations of sheath width due to plasma non-uniformity or instabilities

# Effect of Surface Architecture on Secondary Electron Emission Properties of Materials

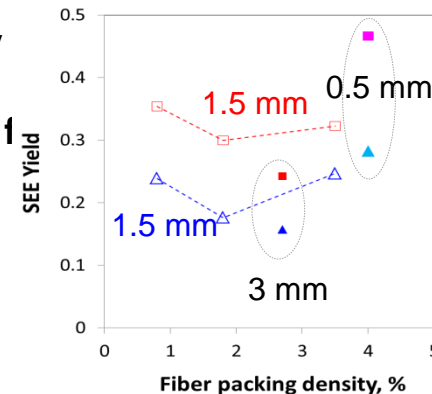
Yevgeny Raitses and Igor Kaganovich



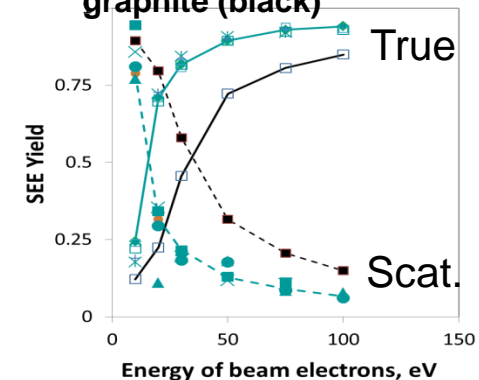
- Strong SEE effects on plasma-wall interaction occur when SEE approaches 1 (top figure).
- For ceramic materials, SEE yield is higher and approaches 1 at lower energies than for metals due to a weaker scattering of SEE electrons on phonons (for insulators),  $\lambda \sim 20$  nm, than on electrons (for metals),  $\lambda \sim 1$  nm.
- Surface-architected materials can reduce the effective SEE yield by trapping SEE electrons between surface structural features.
- The SEE reduction is most significant for high aspect ratio (1:10<sup>3</sup>) velvets than for low aspect ratio (1:10) dendritic coatings (top figure).
- Measurements demonstrate the existence of the optimum aspect ratio and the density of the architectural features (bottom left figure).
- New result: surface architecture affects the energy distribution function of emitted electrons reducing the fraction of backscattered electrons –important for collisionless plasmas used in EP (bottom right figure).



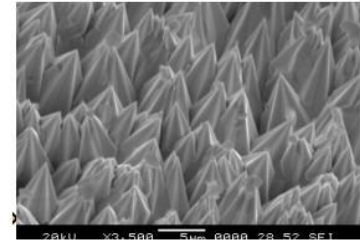
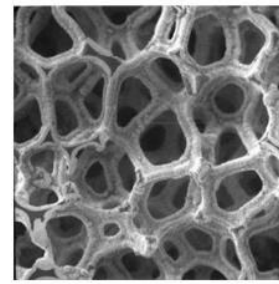
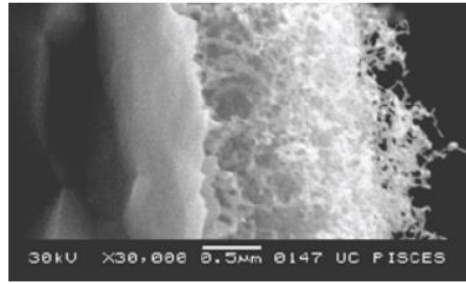
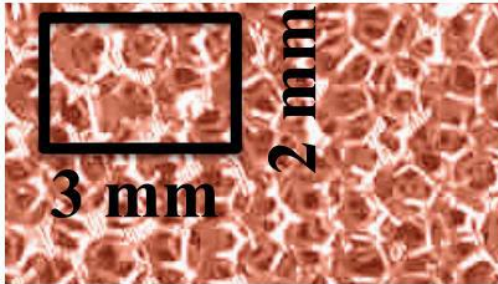
Carbon Velvet: Effect of fiber length and packing density on SEE for beam electrons of 50 eV and



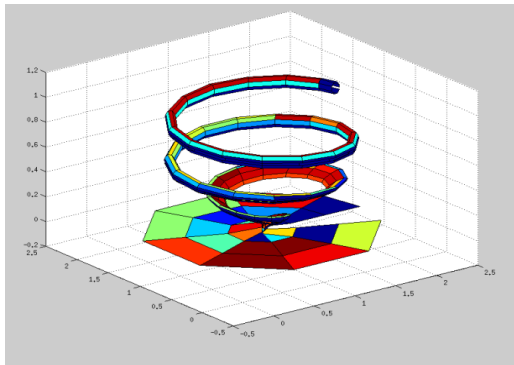
Fractions of true and back scattering SEE electrons measured for velvets (green) and graphite (black)



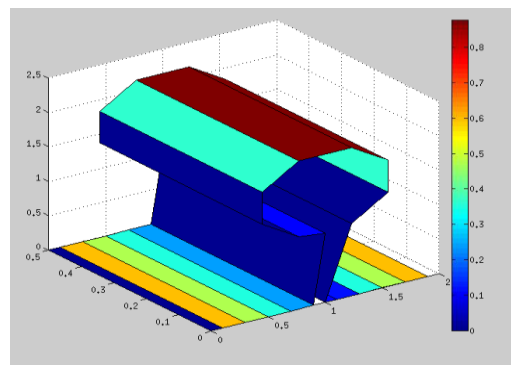
# C. Swanson designed Matlab code to simulate emission from complex surfaces



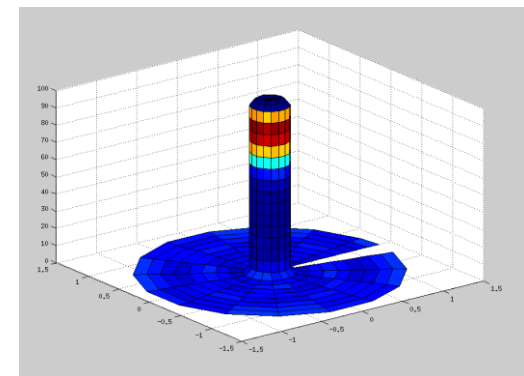
Observed reduction in secondary electron emission yield.



$$\gamma = 0.58 \gamma_{flat}$$



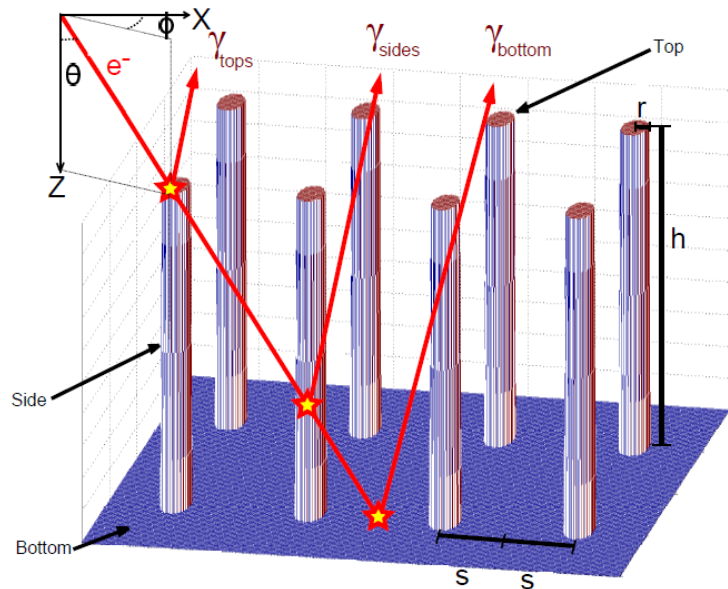
$$\gamma = 0.59 \gamma_{flat}$$



$$\gamma = 0.2 \gamma_{flat}$$

# Calculation of Effective Secondary Electron Emission Yield from Velvet-like structures

Fig.1 Contributions to the SEY emitted by the tops, sides and the bottom surface.



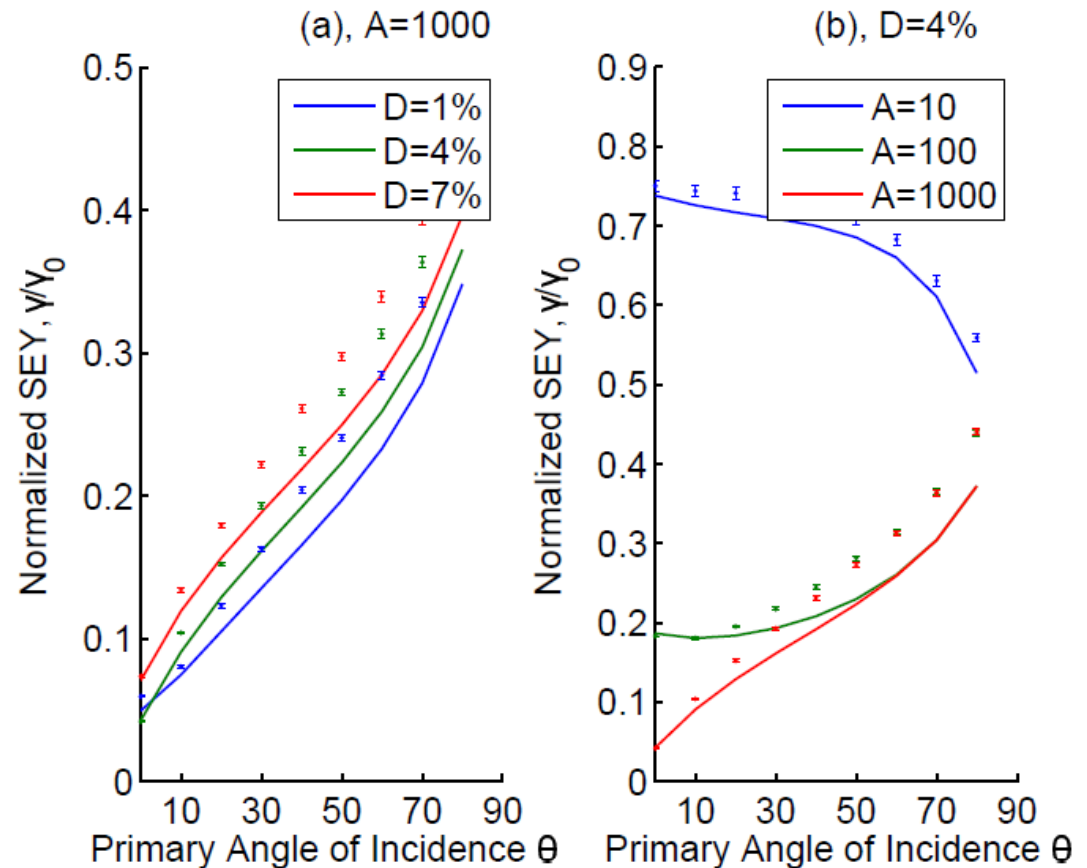
notation of aspect ratio,

$$A = h/r$$

and packing density,

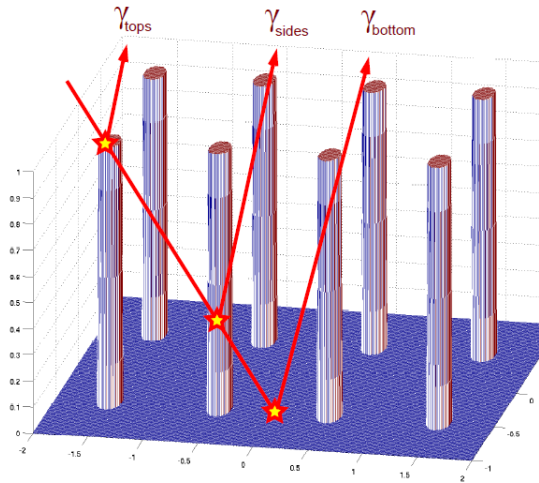
$$D = \frac{\pi r^2}{(2s)^2},$$

Fig.2. SEY vs angle of incidence for different values of aspect ratio,  $A$ , and packing density,  $D$ .



Analytic results vs approximate numerical results for SEY, C. Swanson, I. Kaganovich, submitted to J. Appl. Phys. (2016)

# Analytical Calculation of Effective Secondary Electron Emission Yield from Velvet-like structures (1/2)



*It is apparent from equations 15 and 17 that the dimensionless parameter*

$$u = 2rn\hbar = \frac{2rh}{(2s)^2} = \frac{2}{\pi}DA \quad (18)$$

*is the relevant parameter to characterize a SEE from the velvet surface. The total SEY can be written*

$$\gamma_{eff}(\theta) = \gamma(\theta) [D + (1 - D)f(u, \theta)] \quad (19)$$

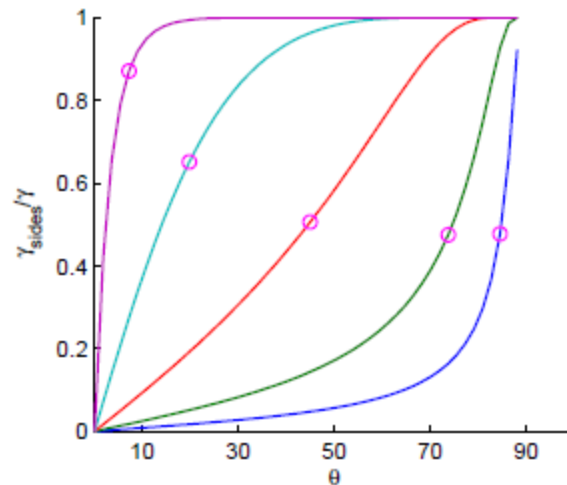
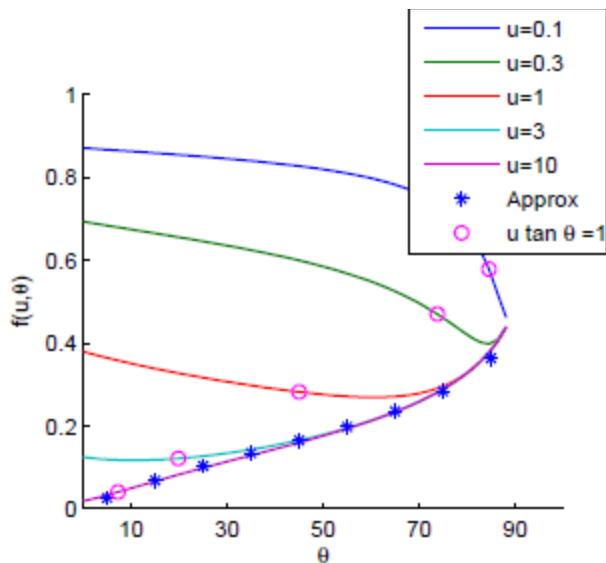
where

$$f(u, \theta) = 2 \int_0^{\infty} dt \frac{te^{-u(t+\tan \theta)}}{(1+t^2)^2} + \frac{\langle \gamma(\theta) \rangle_b}{\gamma(\theta)} \tan \theta \frac{2}{\pi} \int_0^{\infty} dt \frac{t^2}{(1+t^2)^2} \frac{1 - e^{-u(t+\tan \theta)}}{t + \tan \theta} \quad (20)$$

Fig.1 Contributions to the SEY emitted by the tops, sides and the bottom surface.

# Analytical Calculation of Effective Secondary Electron Emission Yield Reduction for Velvet structures (2/2)

FIG. 6. Top:  $f(u, \theta)$  vs  $\theta$  for several  $u$  (curves) that determines the net SEY in equation  $\gamma_{eff} = \gamma_{flat}\{D + (1 - D)f(u, \theta)\}$ , including the approximation given by equation 22 (blue symbols). Bottom: Relative contribution to the SEY of the sides of the whiskers. Pointed out in both are the points at which the quantity  $u \tan \theta$  crosses unity.



$$u = 2rn h = \frac{2rh}{(2s)^2} = \frac{2}{\pi} DA$$

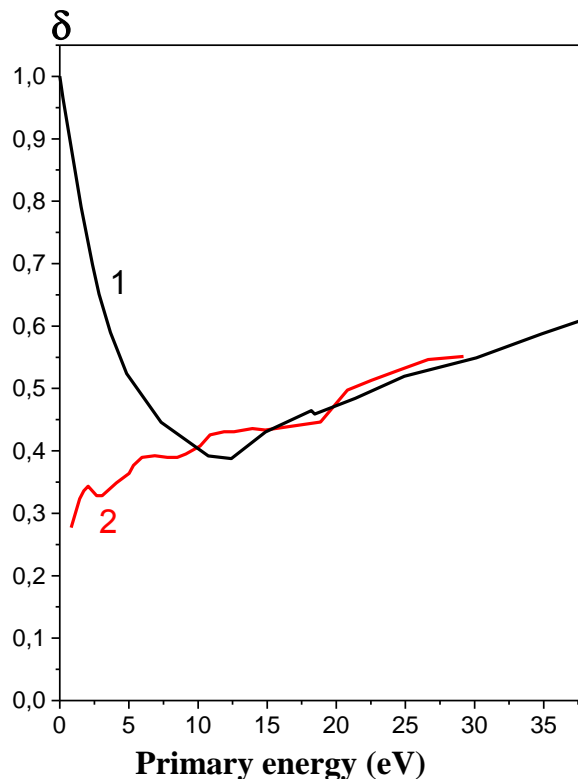
# Outline

---

- Motivation and applications
- Effects of emission on sheath
- Emission from complex surfaces
- **Effect of clean vs “dirty” surface on SEY**
- Two-stream instability in bounded plasmas

# Secondary electron emission at low energy

Total secondary electron yield of Cu as a function of incident electron energy. 1. from the letter for fully scrubbed Cu ( $T=10$  K). 2. Experimental data for bulk Cu after heating in vacuum (room temperature).



1. R. Cimino, et al, Phys. Rev. Lett. **93**, 014801 (2004).
2. I. M Bronshtein, B. S Fraiman. Secondary Electron Emission. Moscow, Russia: Atomizdat, p. 408 (1969).

Other measurements reported the reflection coefficient of about 7% for incident electron energy below few electron volts for most pure metals.

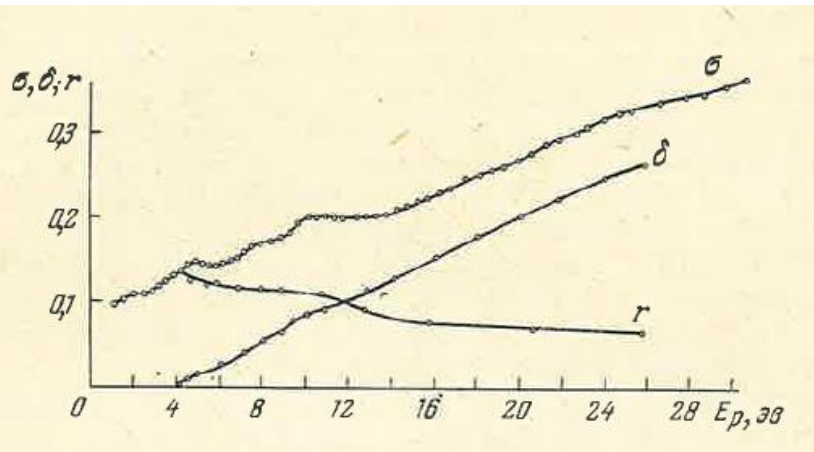
I.H. Khan, J. P. Hobson, and R.A. Armstrong, Phys. Rev. **129**, 1513 (1963).

H. Heil, Phys. Rev. **164**, 887, (1967).

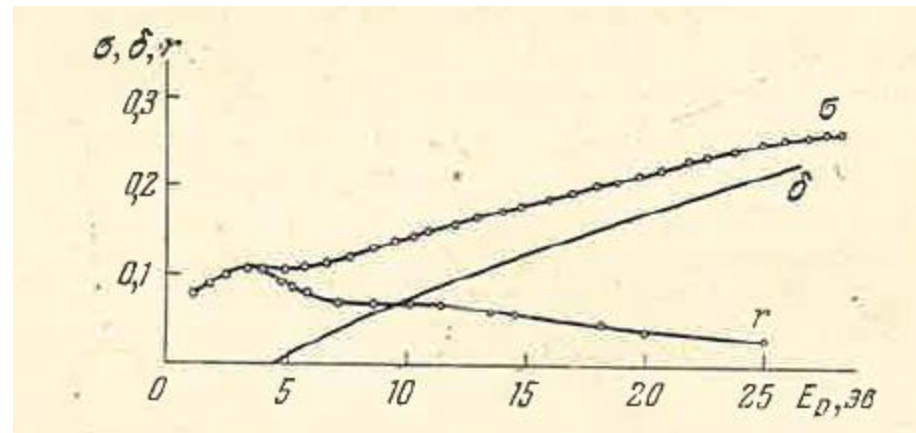
Z. Yakubova and N. A. Gorbatyi, Russian Physics Journal **13** 1477 (1970).

# Previous careful measurements showing contrary observation

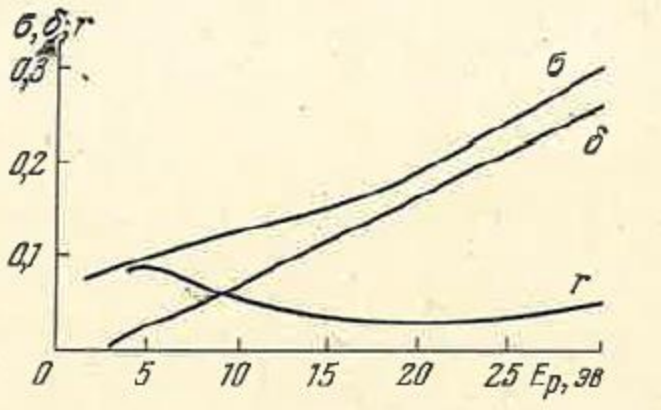
Total secondary electron yield of Al as a function of incident electron energy.



Total secondary electron yield of Ni.



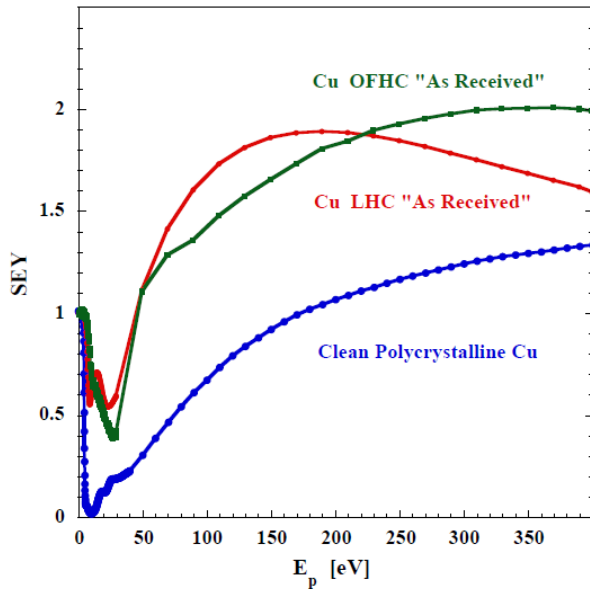
Total secondary electron yield of Si.



I. M Bronshtein, B. S Fraiman. Secondary Electron Emission. Moscow, Russia: Atomizdat, p. 60 (1969).

# Effect of clean vs “dirty” surface on SEY (1/2)

SEY at low energies (<10eV) can be strongly affected by adsorbent gas, see left Fig



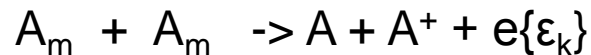
Experimental SEY curves of an Oxygen-free high thermal conductivity (OFHC) polycrystalline Cu "as received" Cu; a LHC "as received" Cu and, for comparison, of a clean polycrystalline Cu as a function of  $E_p$  above  $E_F$ , R. Cimino, et al (2015).



Measurements of low-energy electron reflection at a plasma boundary

V. I. Demidov, S. F. Adams, I. D. Kaganovich, M. E. Koepke, and I. P. Kurlyandskaya

Afterglow plasma can generate monoenergetic electrons via metastable reactions:



Measuring probe on a probe, can then observe the role of surface effects on SEY.

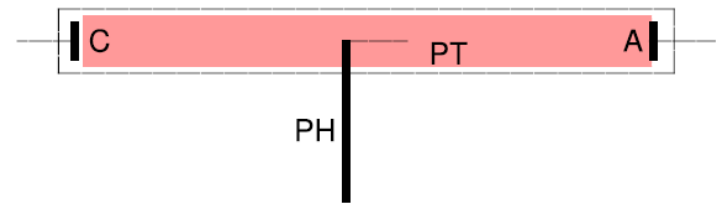
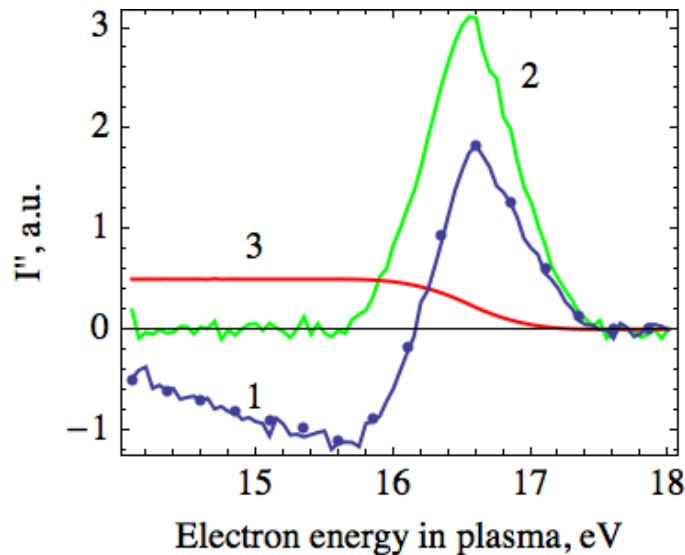


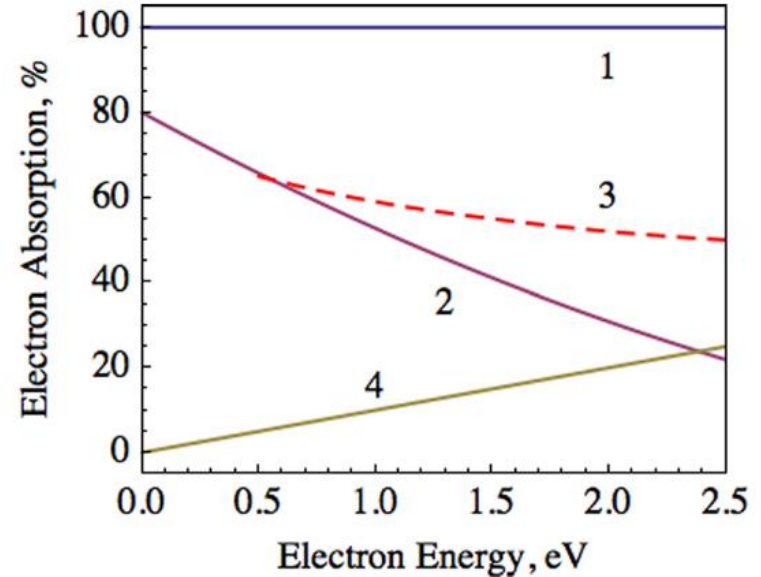
FIG. 3. Schematic of the experimental device. A glass tube has a diameter of 35 mm and length of 30 cm with cold cathode (C) and anode (A). A probe tip (PT) is situated along the tube axis, and probe holder (PH) is perpendicular to the tube axis.

# Effect of clean vs “dirty” surface on SEY (2/2)

SEY at low energies (<10eV) can be strongly affected by adsorbent gas, see left Fig.



Measured second derivative of a probe current for dirty (2) and clean (1) surfaces in neon afterglow plasma. Demidov, et al (2015)



If the probe surface has  $\sigma > 0$ , Eq. (3) has to be modified to take electron reflection into account to become

$$I_d(V) = I_c(V)G(eV), \quad (4)$$

where  $G$  is the absorption coefficient of electrons, averaged over electron incident angles

FIG. 4. Measured electron absorption coefficient,  $G$ , for clean (1) and dirty (2) molybdenum probe surfaces in contact with neon plasma.  $G$  for dirty molybdenum surfaces taken from Ref. 9 (3).  $G$  for cooper surface taken from Ref. 1 (4).

# Outline

---

- Motivation and applications
- Effects of emission on sheath
- Emission from complex surfaces
  - Effect of clean vs “dirty” surface on SEY
- **Two-stream instability in bounded plasmas**

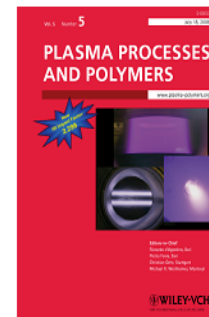
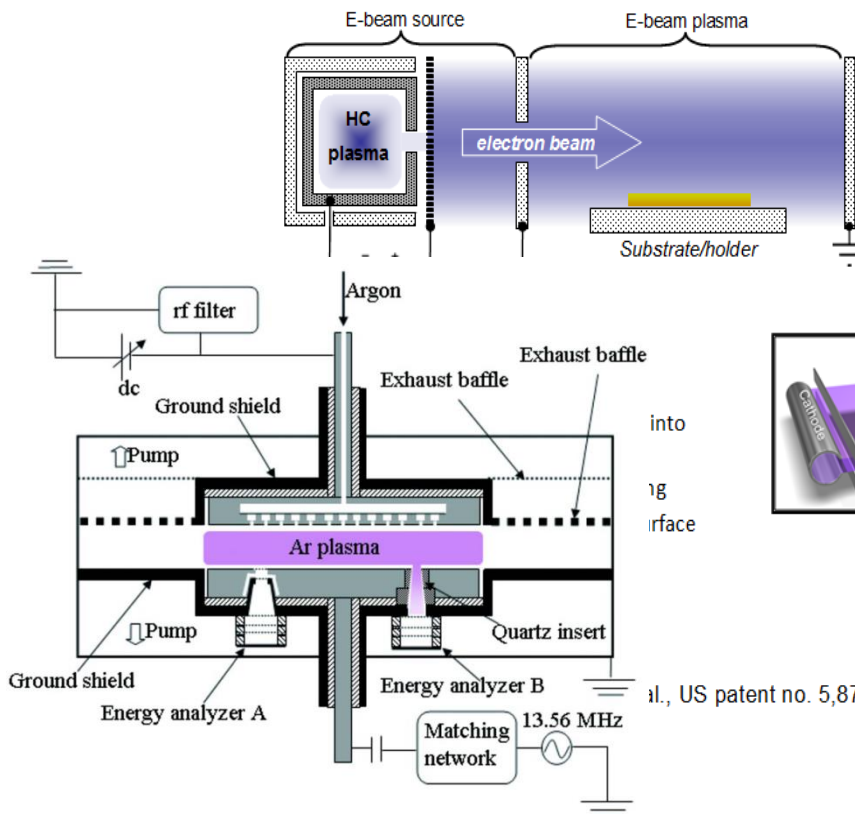
# CONTROLLING PLASMA PROPERTIES BY INJECTION OF ELECTRON BEAM INTO THE PLASMA

## Applications: Plasma Processing Systems, Gas Lasers, Ionization at High Pressures

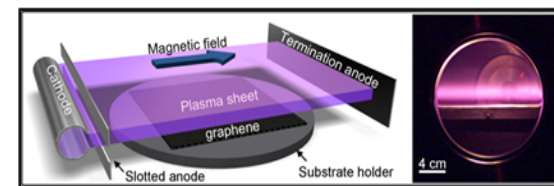
Electron beam generated plasma processing system



### Large Area Plasma Processing System (LAPPS)\*



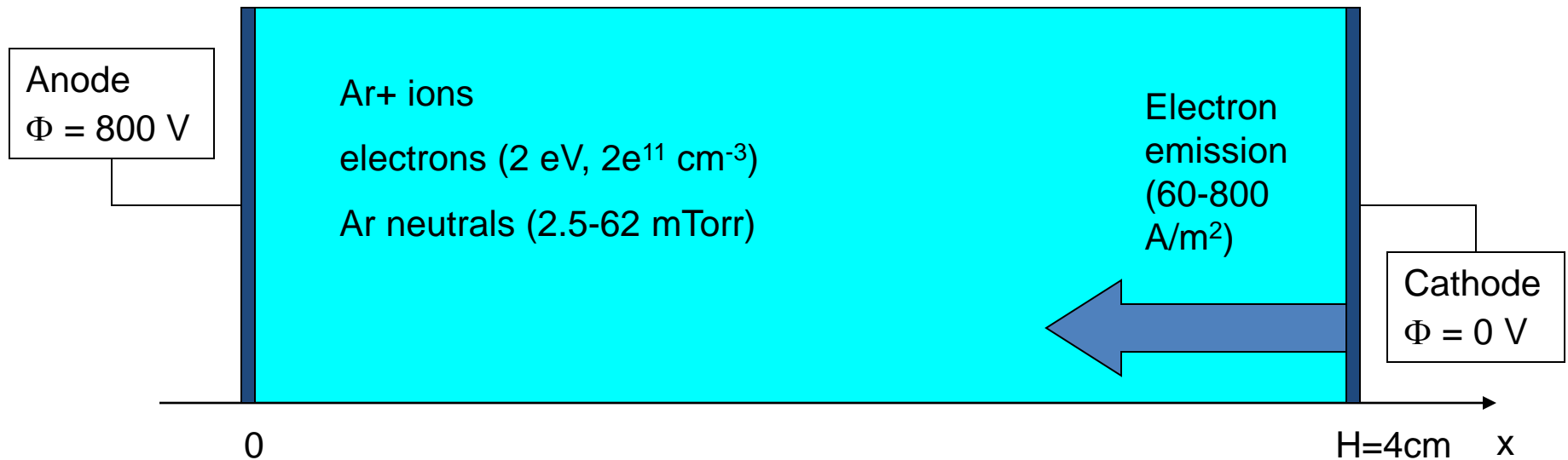
S.G. Walton *et al*, Plasma Proc. and Poly. 5, 453 (2008)



M. Baraket *et al*, App. Phys. Lett. 100, 233123 (2012)

al., US patent no. 5,874,807 (Feb. 1999)

# DC SYSTEM SIMULATED WITH EDIPIC



**Magnetic field turned off.**

**External electric field parallel to the walls turned off.**

**Elastic and inelastic collisions are on, **ionization is off.****

**Numerical grid ~ 5000 cells.**

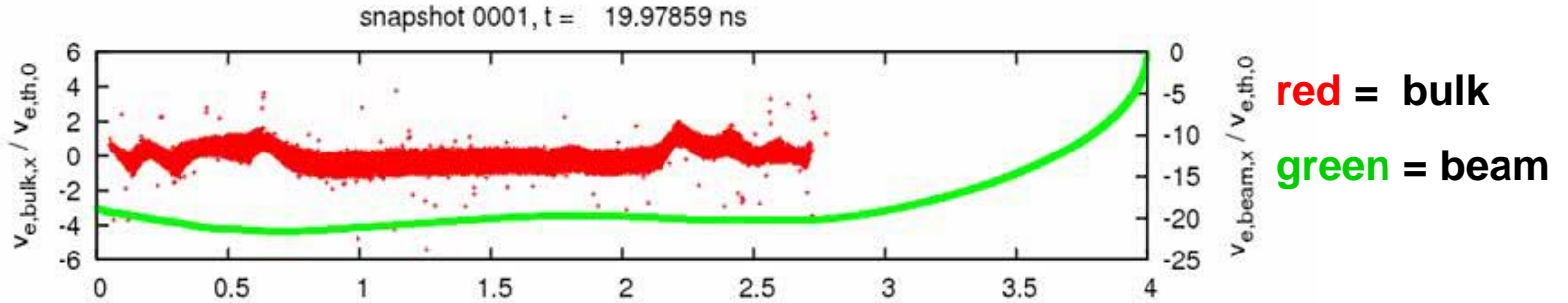
**Cell size is few  $\mu\text{m}$ .**

**Time step sub ps.**

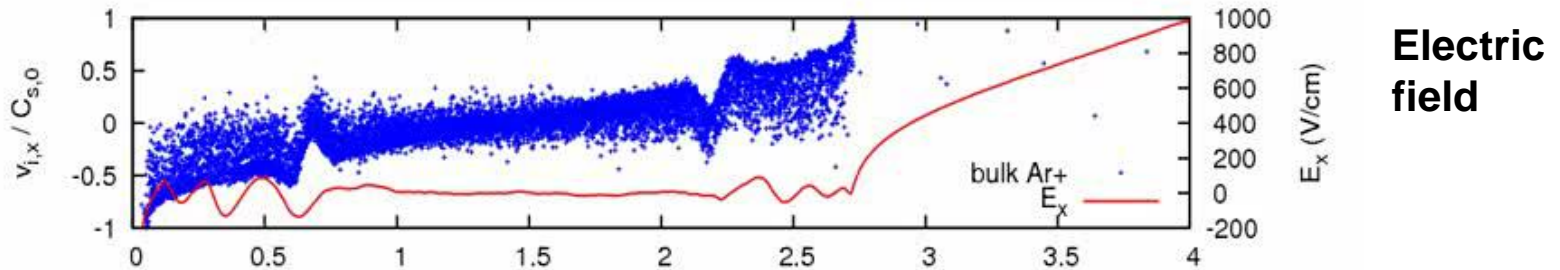
**Initial number of macroparticles is 10 mlns**

# SIMULATION OF MULTI-PEAK ELECTRON VELOCITY DISTRIBUTION FUNCTION

Electron velocity

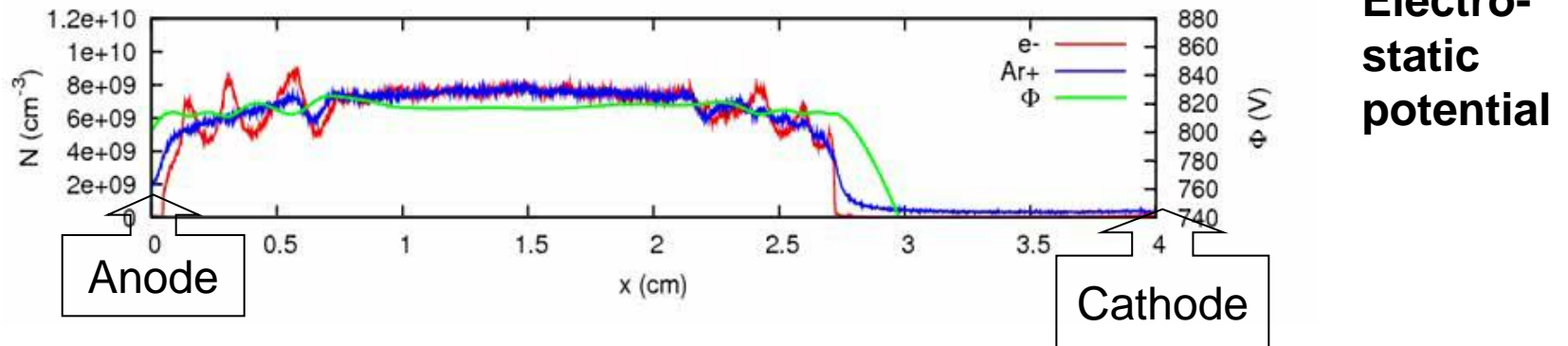


Ion velocity



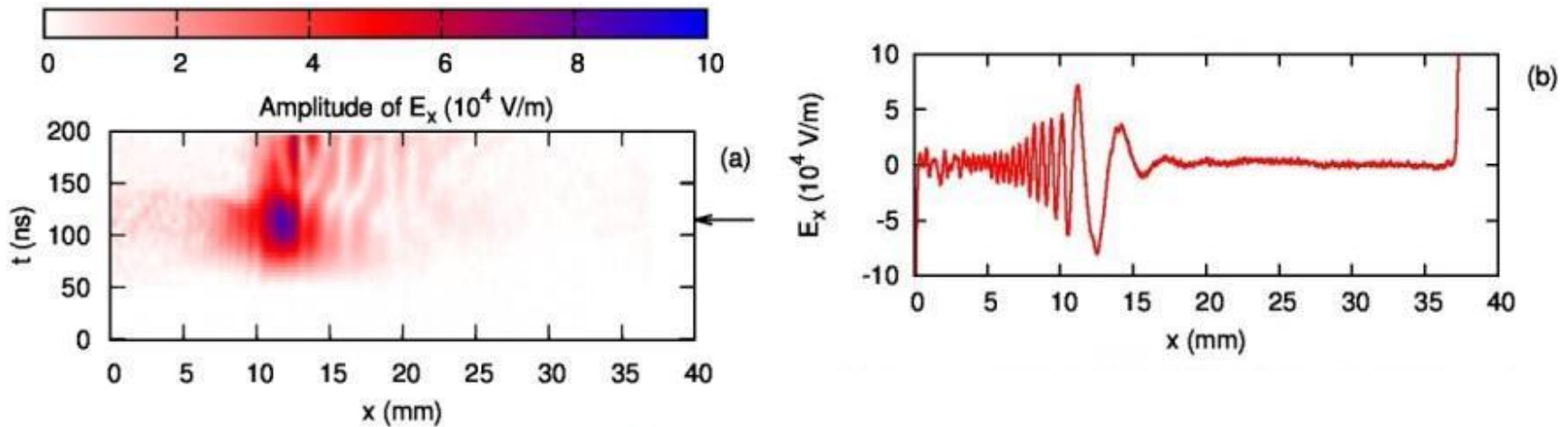
Electric field

Density



Electrostatic potential

# ELECTRIC FIELDS CAN REACH kV/cm WITH BEAM CURRENT OF 20 mA/cm<sup>2</sup>

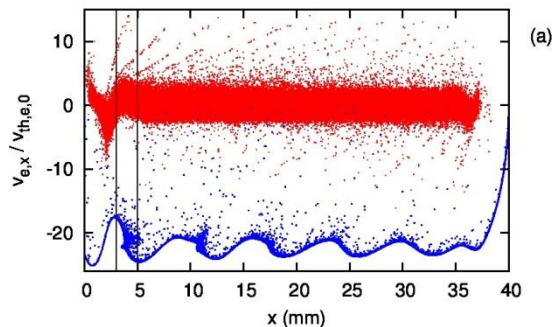


Now there is sufficient “kick” from the electric field to accelerate electrons out of the background.

# SIGNIFICANT ACCELERATION OF BULK ELECTRONS

Snapshot 1, lowered frequency regime

Electron bulk (red) and beam (blue) phase plane



EVDF of bulk (red) and beam (blue) electrons

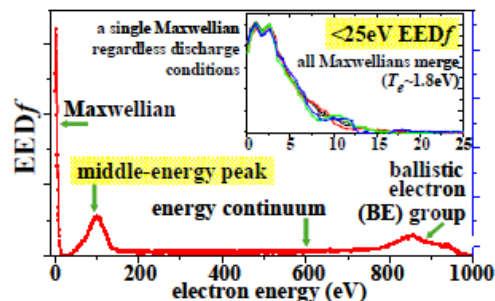
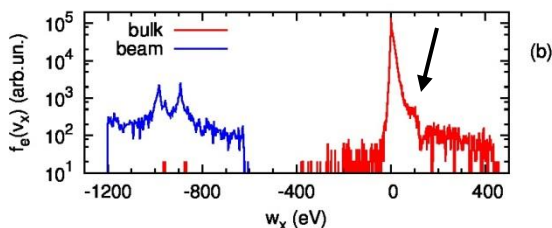
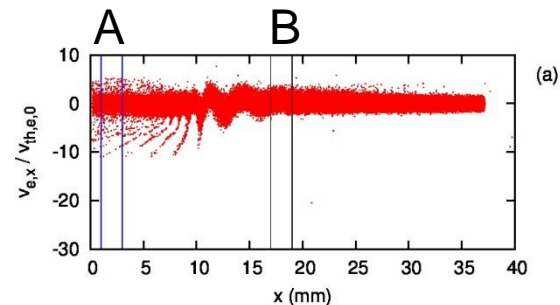


Fig. 1. Non-Maxwellian EEDF of DC/RF plasma.

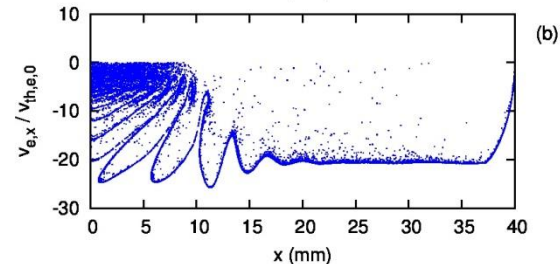
From [Chen and Funk, 2010].

Snapshot 2, ordinary regime

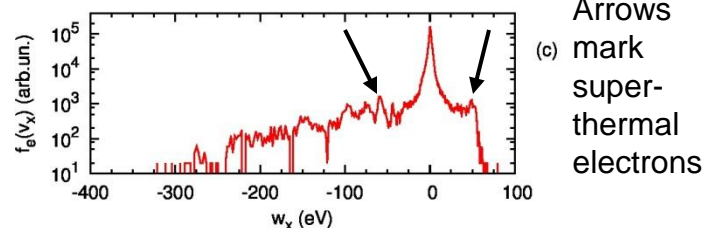
Electron bulk phase plane



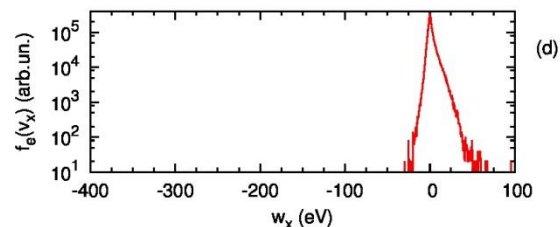
Emitted electrons phase plane



EVDF of bulk electrons in area A



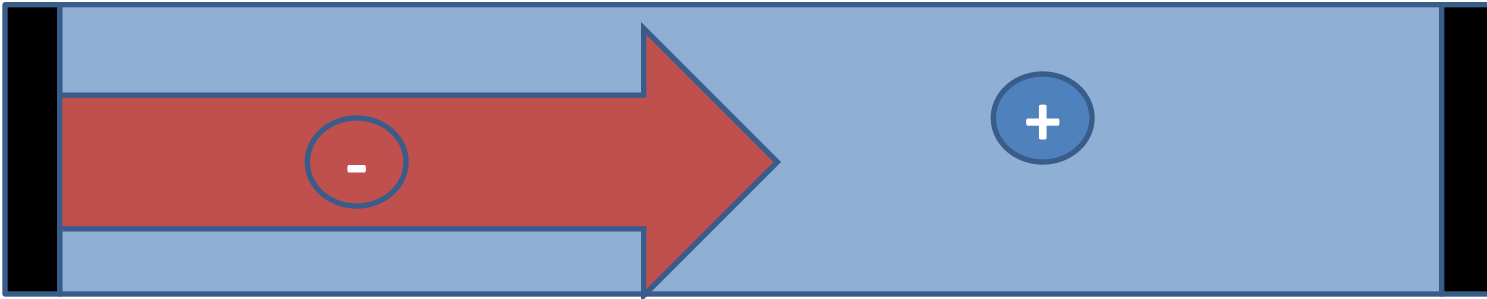
EVDF of bulk electrons in area B



**We developed analytical theory for threshold of instability as function of plasma parameters and collisions**

# PIERCE MODEL (1944)

---



Electron beam is injected into ion background of equal density to the electron beam.

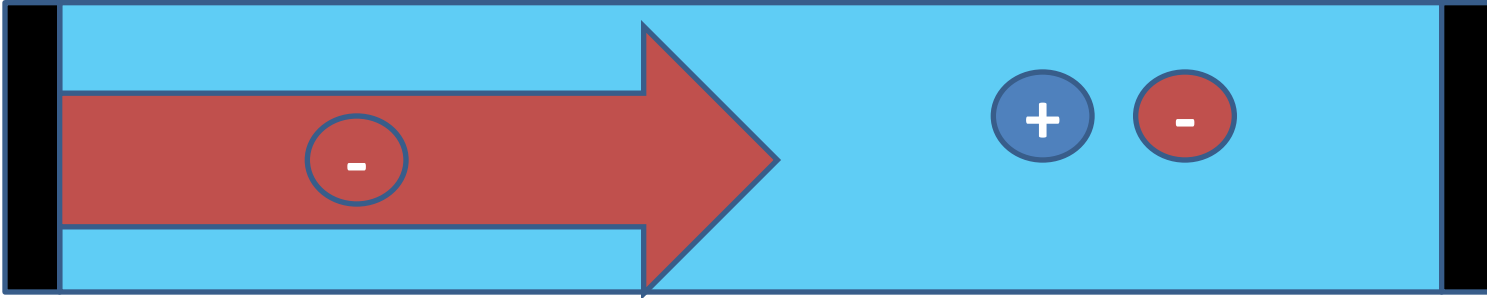
Electrodes with fixed potential set potential at boundaries.

Instability develops if  $\omega_{pb} L / v_b > \pi$

This limits the current propagation through the gap.

# OUR MODEL (2015?)

---



Electron beam is injected into electron and ion background of equal density.

Electrodes with fixed potential set potential at boundaries.

Instability is very different from textbook calculation for periodic b.c.

$$\omega_{e,0} (n_{b,0}/n_{e,0})^{1/3}$$

# ANALYTIC SOLUTION

---

$$\frac{\partial n_{e,b}}{\partial t} + \frac{\partial v_{e,b} n_{e,b}}{\partial x} = 0 \quad \delta n_b(0) = \delta v_b(0) =$$

$$\frac{\partial v_{e,b}}{\partial t} + v_{e,b} \frac{\partial v_{e,b}}{\partial x} = -\frac{e}{m} E \quad \delta \phi(0) = \delta \phi(L) = 0$$

$$\delta \phi(t, x) = (Ax + Be^{ik_+x} + Ce^{ik_-x} + D) e^{-i\omega t},$$

the following additional relation between  $\omega$  and  $k$ :

$$k_-^2 (e^{ik_+L} - 1) - \frac{ik_-^2 k_+ \omega L}{\omega - k_+ v_{b,0}} =$$

$$k_+^2 (e^{ik_-L} - 1) - \frac{ik_+^2 k_- \omega L}{\omega - k_- v_{b,0}} \quad \rightarrow \quad -i \frac{2(1-\chi)}{(1+\chi)\chi} L_n + e^{i(1-\chi)L_n} - 1 -$$

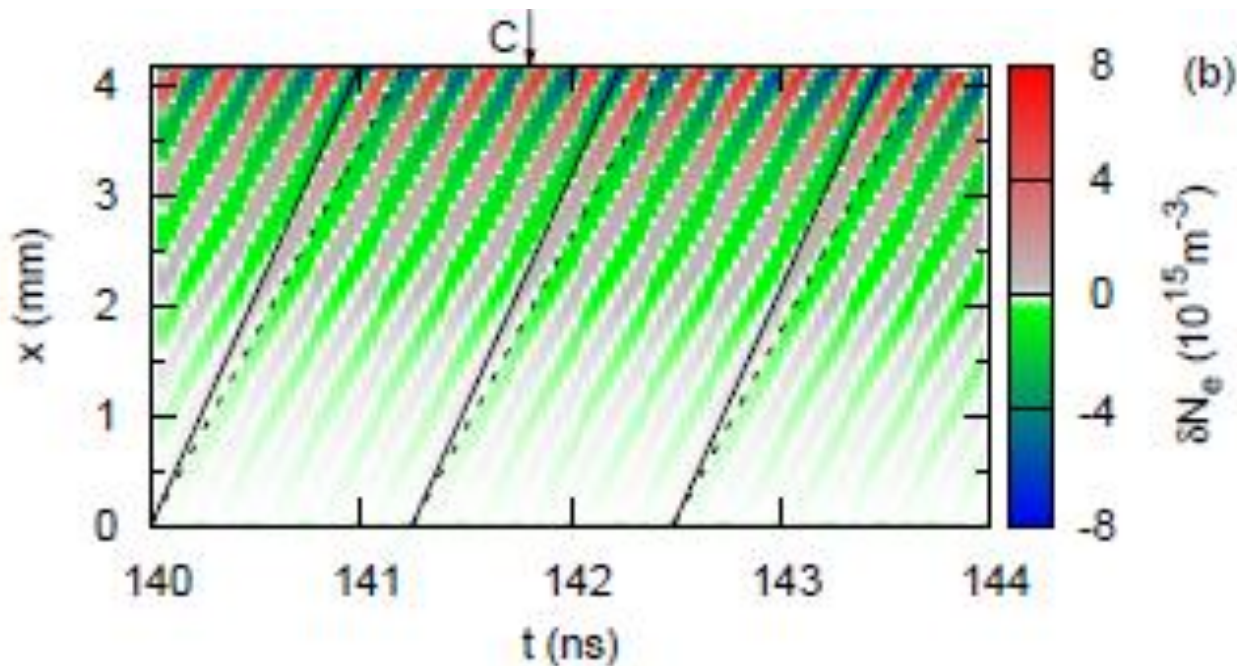
$$k_{\pm} = (1 \mp \chi) \frac{\omega_{e,0}}{v_{b,0}} \quad \frac{(1-\chi)^2}{(1+\chi)^2} \left[ e^{i(1+\chi)L_n} - 1 \right] = 0$$

(10)

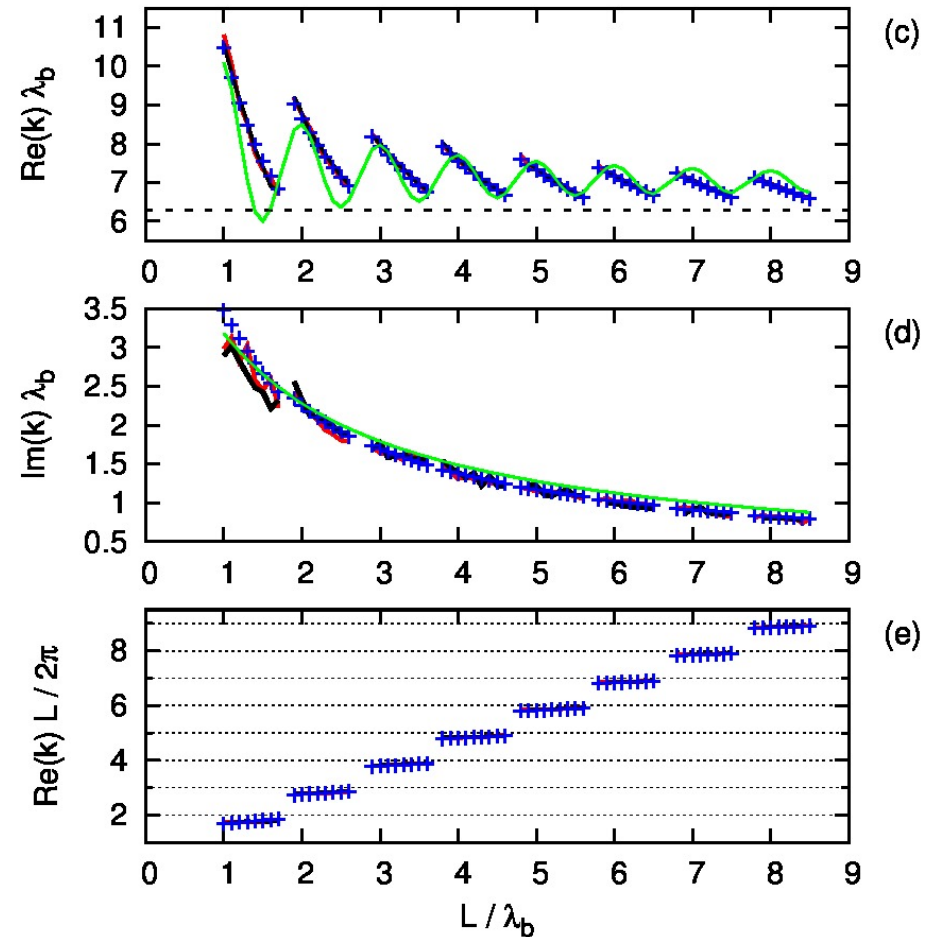
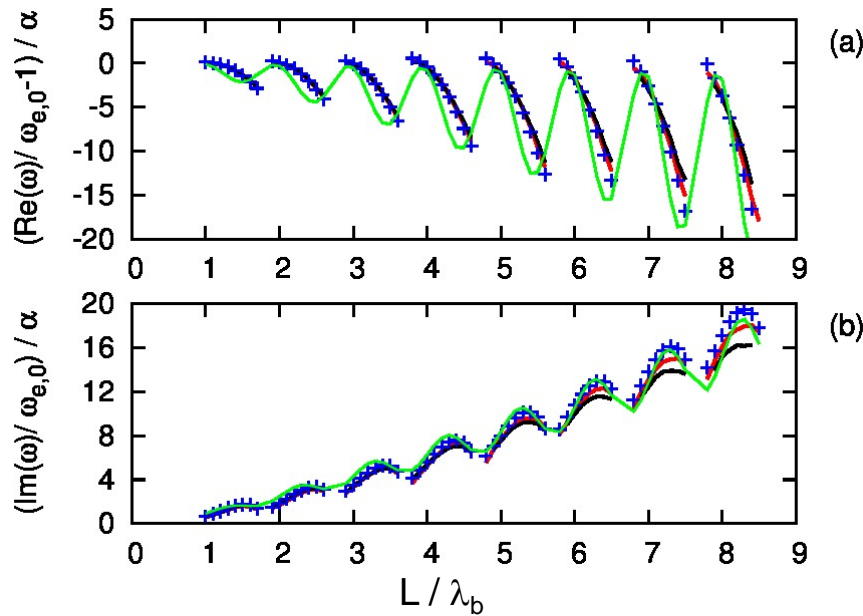
# RESULTS: MODE IS SPATIALLY GROWING

---

Evolution of the bulk electron density perturbation in time and space in fluid; Solid black lines in represent propagation with the unperturbed beam velocity. Dashed black lines in represent phase velocity of the wave calculated analytically.



**Frequency (a), temporal growth rate (b), wavenumber (c), spatial growth rate (d), and the number of wave periods per system length (e) versus the length of the system.**



The blue crosses mark values obtained by analytical solution.

$$\text{Im}(\omega) \approx \frac{1}{13} L_n \ln(L_n) \left[ 1 - 0.18 \cos\left(L_n + \frac{\pi}{2}\right) \right] \alpha \omega_{pe},$$
 where  $L_n = L \omega_{pe} / v_b$ , wavenumber  $\text{Re}(k) \approx \frac{\omega_{pe}}{v_b} \left[ 1 + \frac{1 + 2.5 \cos(L_n)}{1.1 L_n} \right]$ . For comparison, the classical values: growth rate  $\text{Im}(\omega) = 0.7 \alpha^{1/3} \omega_{pe}$ .

Solid red and black curves represent values obtained in fluid simulations with  $\alpha = 0.00015$  (red) and  $0.0006$  (black). Solid green curves are values provided by fitting formulas. In (c), the black dashed line marks the resonant wavenumber.

# EFFECT OF COLLISIONS ON THE TWO-STREAM INSTABILITY IN A FINITE LENGTH PLASMA

Collisions of plasma bulk electrons further reduces this growth rate. The rate becomes zero if the collision frequency is equal to the doubled growth rate without collisions.

$$Im(\omega) = Im(\omega_{ncl}) - \nu_e/2 .$$

$$Im(\omega_{ncl}) \approx \frac{1}{13} L_n \ln(L_n) \left[ 1 - 0.18 \cos \left( L_n + \frac{\pi}{2} \right) \right]$$

$$J_{b,thr} = \frac{6.5\kappa(T_e) \sqrt{2e\epsilon_0 n_{e,0} W_{b,0}}}{L_n \ln(L_n) [1 - 0.18 \cos(L_n + \pi/2)]} p_n$$

Pressure should be less than  $P=15\text{mTorr}$  for the beam current  $J_{b,thr} = 5.4\text{mA/cm}^2$  to observe the instability.

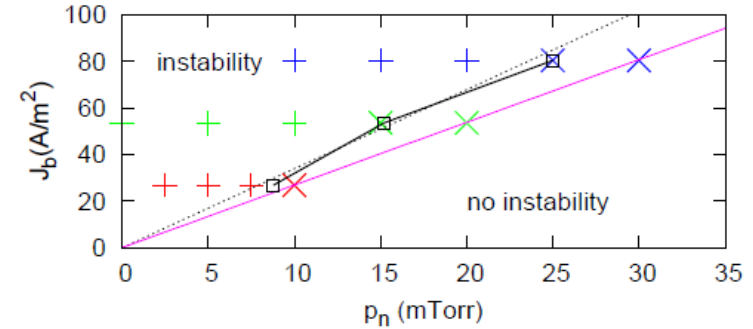


**FIG. Phase plane “emission current density vs neutral gas pressure”.** The dashed black straight line is the analytical threshold current plotted using these threshold pressure values.

$n = 2 \cdot 10^{11} \text{ cm}^{-3}$ ,  $L = 1.85\text{cm}$ ,  
Beam energy = 800 eV.

# CONCLUSIONS

---

- **SEE is important to take into account for many applications with  $T_e > 20\text{eV}$  for dielectrics and  $T_e > 100\text{eV}$  for metals.**
- **SEE strongly affects sheath.**
- **Instability and inverse sheath were observed due to EVDF-sheath coupling.**
- **Complex structures can reduce secondary electron emission yield (SEY). Theory was developed for optimal velvet parameters to reduce SEY.**
- **Absorbed layer can strongly affect SEY and the effect was measured using probe in discharge of noble gases using Penning reaction that produces monoenergetic fast electrons.**
- **SEE can create beams of electrons penetrating the plasma, beam-plasma interaction can cause a two-stream instability. We have studied the development of the two-stream instability in a finite size plasma bounded by electrodes both analytically and making use of fluid and particle-in-cell simulations. Its behavior is very different from infinite plasma.**